Nanoscale Horizons
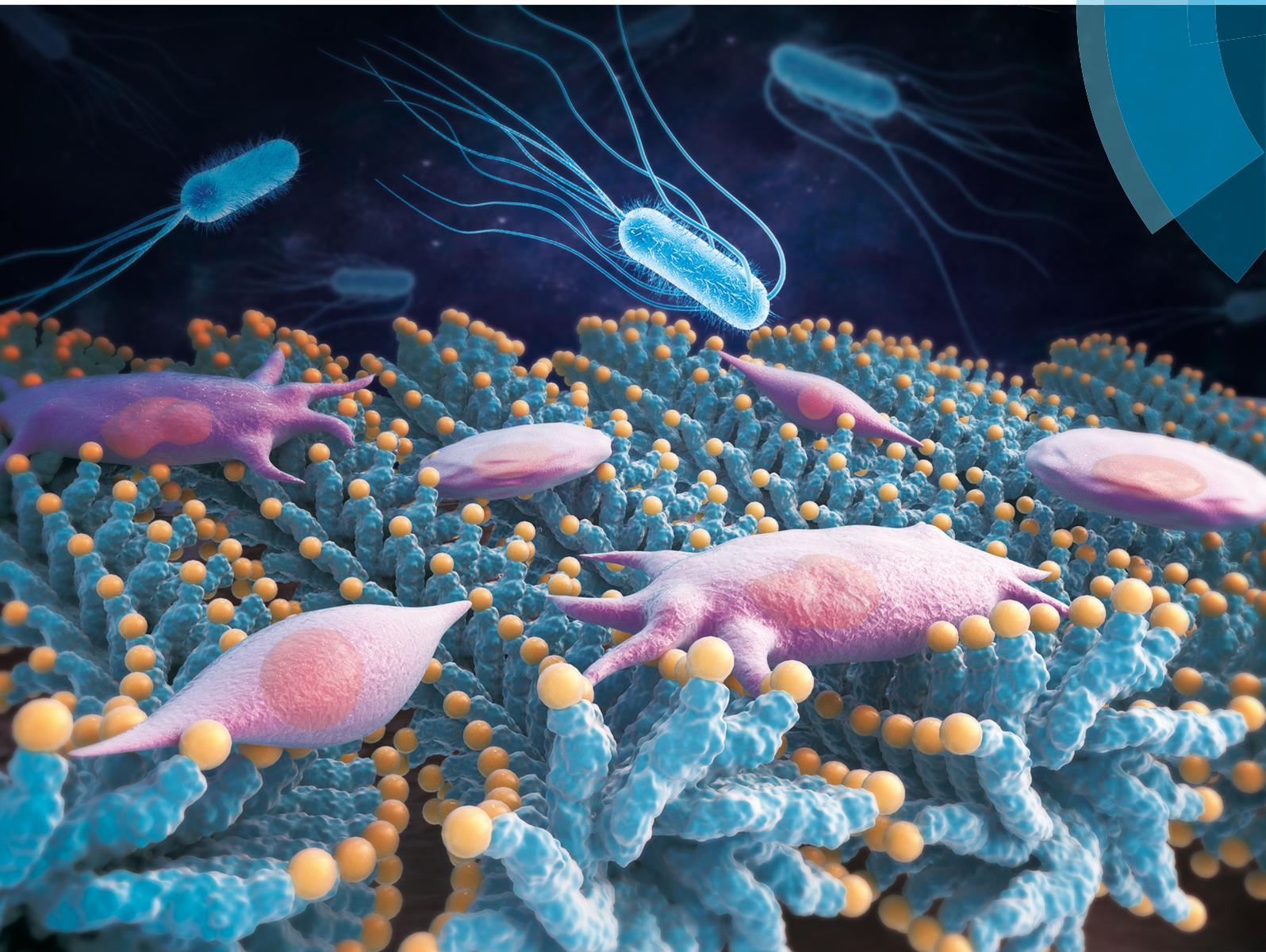
The home for rapid reports of exceptional significance in nanoscience and nanotechnology

rsc.li/nanoscale-horizons

ROYAL SOCIETY OF CHEMISTRY | Celebrating IYPT 2019

COMMUNICATION
Chuanbin Mao *et al.*
Bacterial flagella as an osteogenic differentiation nano-promoter

NCNST

Check for updates

Bacterial flagella as an osteogenic differentiation nano-promoter†

Dong Li,[a] Ye Zhu,[a] Tao Yang,[b] Mingying Yang[c] and Chuanbin Mao ID *[a]

Flagella as protein nanofibers (∼14 nm wide) on the surface of swimming bacteria are molecular machines for assisting bacteria to swim in the liquid. They are mainly assembled from protein subunits (FliC) that can be genetically engineered to display peptides. However, so far, no study has been made to show whether flagella with or without displaying peptides could direct stem cell fate. Here we show that flagella detached from bacteria could promote the osteogenic differentiation of bone marrow derived mesenchymal stem cells (BMSCs), and the display of a functional peptide and mineralization of bone mineral (hydroxylapatite, HAP) on the flagella further collectively enhance the promotion effect. The functional peptide is made of two fused amino acid sequences, RGD and E8, which are responsible for promoting cell adhesion onto flagella-bearing substrates and inducing HAP mineralization on flagella from an HAP-supersaturated solution, respectively. Our work shows that the unique nanotopography and surface chemistry of both mineralized and non-mineralized flagella enable them to present physical and chemical cues favoring the osteogenic differentiation of stem cells. Thus flagella are nanofibrous osteogenic differentiation promoters that can be used to build extracellular matrix-like materials.

New concepts

Stem cells need to be specifically differentiated into bone forming cells (*i.e.*, osteoblasts) for successful bone regeneration. However, stem cells naturally differentiate into multiple cells randomly. Thus a nanostructured material is needed to promote their differentiation into osteoblasts. Currently reported nanostructured materials usually do not bear the possibility of genetic modification that is desired in precisely displaying a signaling peptide. Here for the first time, we discover that protein nanofibers used as a molecular machine to enable bacteria to swim, called flagella, could promote the differentiation of stem cells into osteoblasts. Flagella are helically assembled from genetically modifiable protein subunits. When the flagella are genetically modified to bear cell-signaling molecules or chemically modified with bone minerals, the flagella become more capable of promoting the differentiation. Since bacteria naturally grow flagella on their surface, which can be purified, the discovery of flagella being a differentiation nano-promoter provides a cost-effective new nanomaterial that can either fill the bone defects as a scaffold or modify the implant surface as a film to enhance bone regeneration to repair bone defects. This work also suggests that the flagella can be used to control the stem cell differentiation due to their unique morphology and surface chemistry.

Introduction

Due to their versatile chemistry, molecular recognition properties and biocompatibility, peptide and protein based nanomaterials gained much attention in directing cell fates.[1–6] Nanostructured biomaterials with cell-favorable surface properties promote cell fates since cells directly interact with the nanostructured extra-cellular matrix (ECM) in the development of tissues such

as bone.[2] Many biomolecular materials, such as collagen, chitosan, silk proteins, peptide amphiphiles and bacteriophages,[7–12] have been employed for the synthesis of bone-like ECM. Bone ECM is not a simple mixture of organic (mainly collagen) and inorganic (mainly hydroxylapatite, HAP) phases but has a unique spatial relation with respect to each other. At nanometer level, collagen molecules self-assemble into parallel collagen fibrils and HAP nanocrystals are nucleated along the collagen fibrils.[13] Thereafter, use of a protein nanofiber to nucleate HAP is a feasible approach to the formation of an HAP-mineralized collagen fibril-like nanofiber.[14] The synthesis should take place under mild conditions such as at room temperature and in aqueous solution.

In this study, a naturally occurring protein nanofiber, bacterial flagellum, which is orderly assembled from several thousand copies of monomers called flagellin (*FliC*), is employed for the display of functional peptide and nucleation of HAP nanocrystals on the surface. *FliC* is synthesized inside bacteria and then

[a] *Department of Chemistry and Biochemistry, Stephenson Life Sciences Research Center, Institute for Biomedical Engineering, Science and Technology, University of Oklahoma, Norman, Oklahoma 73072, USA. E-mail: cbmao@ou.edu*

[b] *School of Materials Science and Engineering, Zhejiang University, Hangzhou, Zhejiang 310027, P. R. China*

[c] *Institute of Applied Bioresource Research College of Animal Science, Zhejiang University, Yuhangtang Road 866, Hangzhou 310058, China*
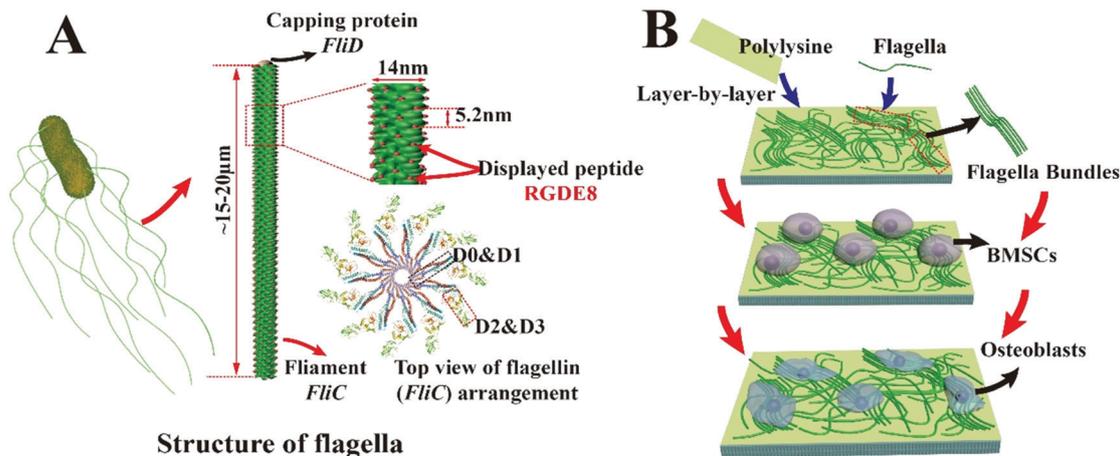
† Electronic supplementary information (ESI) available. See DOI: 10.1039/c9nh00124g

Scheme 1 Schematic illustration of peptide display on flagella, purification of flagella from bacteria surface, and growth and differentiation of bone marrow derived mesenchymal stem cells (BMSCs) on the flagella-based substrates. (A) Structure of flagella. The surface-exposed portion (D2 & D3 domain) can be genetically engineered by insertion of a foreign peptide (RGDE8), leading to the peptide display on the surface of flagella. After the peptide is displayed on the flagella, the flagella can be purified from the bacteria surface by a simple vortexing. (B) Formation of the flagella substrates from flagella (mineralized or non-mineralized) using a layer-by-layer method. The positively charged polylysine initiates the first layer of the substrate followed by the deposition of the negatively charged flagella layer. After several cycles of deposition, the top surface is terminated with a layer of flagella. Then, BMSCs are seeded on this substrate under osteogenic conditions. With the help of nanotopographic surfaces and surface chemistry generated by bioengineered flagella, BMSCs finally differentiate into osteoblasts.

assembled on the surface of bacteria into flagella. The resultant flagella can also be detached from bacteria by simple vortexing and isolated by ultracentrifugation, allowing us to genetically engineer and physically purify flagella. The flagellar nanofiber has an outer and inner diameter of ~ 14 and 2 nm, respectively, and a length up to several microns.[15,16] The N- and C-terminal domains of *FliC* (D0 and D1) are highly conserved; on the contrary, the central regions (D2 and D3) are hyper variable and thus can be modified by the insertion or deletion of sequences without losing its self-assembly properties (Scheme 1A).[17] Here a peptide, RGDEEEEEEEE (RGDE8), fused from two peptide motifs, the integrin-binding motif Arg-Gly-Asp (RGD) as a cell-adhesion peptide (commonly seen in collagen and other ECM proteins) and 8 contiguous Glu residues (E_8, which is an HAP-nucleating domain in a non-collagenous bone protein called bone sialo-protein),[18] was displayed on the hyper variable solvent-exposed exterior surface of flagella. Then we used the RGDE8-displayed flagella to induce HAP mineralization from an HAP-supersaturated solution and form a mineralized nanofibrous matrix mimicking some aspects of the bone ECM. We discovered that the flagella-bearing matrix promoted the adhesion, proliferation and osteo-genic differentiation of bone marrow derived stem cells (BMSCs) for the first time (Scheme 1B).

Results and discussions

The distance between adjacent *FliC* subunits on the highly ordered surface of flagella is about 2.6 nm,[15] resulting in the similar periodicity of the bioactive RGD motif on the flagellar surface introduced by flagellar display (Scheme 1A). A high density of about 3.43×10^4 epitopes per μm^2 can thus be

constructed on the flagellar surface. Surface topography on the material surface especially nanotopography is another important factor that can trigger signaling cascades to modulate cell behaviour.[2,7] Thus we studied the synergistic effect of nanotopo-graphy (contributed by mineralization and assembly of flagellar filaments) and surface chemistry (due to the peptide display and mineral formation on the flagellar surface) on the proliferation and osteogenic differentiation of BMSCs.

Peptides and proteins are important in controlling the bio-mineralization of hard tissue. The negatively charged amino acids, especially the E_8, are known to be the main factor to attract calcium ions followed by HAP formation.[18,19] Biomimetic mineralization has been considered one of the promising approaches for the fabrication of inorganic nanoparticles[20] and bone-like bio-materials.[21] During the flagella production process, RGDE8-displayed flagellins expressed in the bacteria were transported to the outer surface of the bacteria and *in situ* assembled into RGDE8-displayed flagella on the surface of bacteria. Then the bacteria were vortexed to detach the flagella from them and the flagella were further purified from the resultant mixture through centrifugation. The RGDE8-displayed flagella were then allowed to be mineralized in a 4 mM supersaturated HAP solution (prepared following our previous protocol[22,23]) for 6 days at room temperature. We found that the bioengineered flagella could mediate the nuclea-tion of HAP nanocrystals (Fig. 1A and 2). The biomineralized RGDE8 flagella were deposited on the polylysine substrate by a layer-by-layer (LBL) assembly technique. Purified RGDE8 flagella (4.264 µg µl^{-1}) exhibited a characteristic curly morphology when air-dried on the polylysine substrate (Fig. 1A, left). After HAP mineralization, RGDE8-displaying flagellar filaments were coated by a layer of mineral and became relatively "straight" (Fig. 1A, middle). Interestingly, at some areas, the mineralized flagella are assembled into
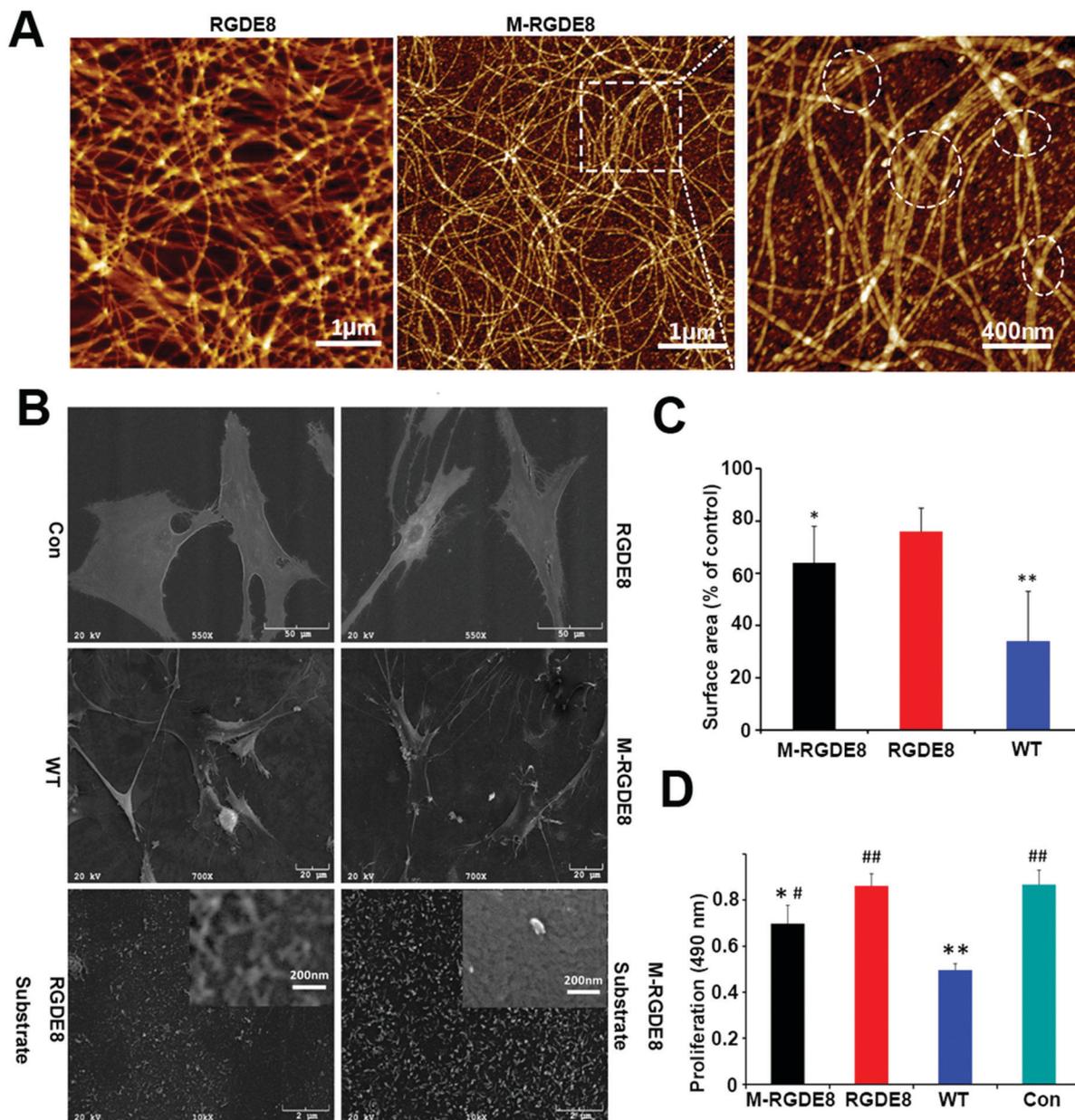
Fig. 1 Morphology of engineered and mineralized flagella substrates and BMSCs as well as evaluation of adhesion and proliferation of BMSCs on the substrates. (A) AFM micrographs of nanotopography surfaces generated by bioengineered flagella. After mineralization, bundle-like flagella are observed and marked by dashed circles. (B) SEM micrographs of BMSCs. Cells spread well on polylysine (Con); Cells spread less on RGDE8 flagella (RGDE8) and much less on wild-type flagella (WT); On the HAP-mineralized RGDE8 flagella (M-RGDE8), BMSCs spread less but show more and longer filopodia-like extensions. Bioengineered flagella (RGDE8) coated surface (high magnification, inset) show fibrous structures which could be formed by flagella or small bundles of flagella. After mineralization, the surface becomes rougher. (C) The cells surface area is substrate dependent. BMSCs exhibit much low surface area on WT. After RGD is displayed on flagella, surface area of BMSCs is increased (compared with control group,$* p < 0.05$, $** p < 0.01$). (D) Proliferation of BMSCs on RGD-displayed flagella surface is faster than that on WT flagella. After mineralization (M-RGDE8), the cell growth rate is decreased (compared with control group, $* p < 0.05$, $** p < 0.01$; compared with WT group, $\# p < 0.05$, $\#\# p < 0.01$).

parallel bundle-like structures (Fig. 1A and 2), mimicking some key structural features of mineralized collagen fibrils. In natural bone, the mineralized collagen fibrils are also parallel-aligned to generate organized nanostructures.

We then studied the stem cell behaviors on four types of substrates, including RGDE8-displaying flagella (RGDE8), bio-mineralized RGDE8 flagella (M-RGDE8), wild-type flagella (WT),

and polylysine as the control (Con). After being seeded on the substrates for 24 h, BMSCs showed a characteristic fibroblastic morphology (bipolar to polygonal). They spread better on RGDE8 and M-RGDE8 flagella than on WT flagella (Fig. 1C and Fig. S1, ESI†). On WT flagella, BMSCs spread much less and some of the cells exhibited a round-like morphology, indicating less favorable adhesion due to the lack of RGD. However, BMSCs could still
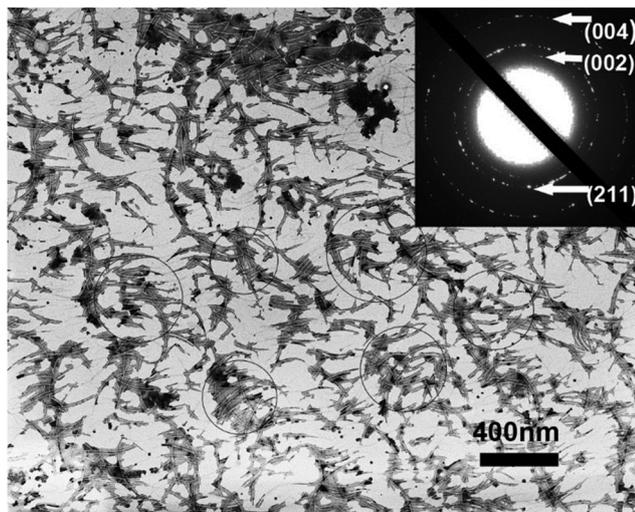
Fig. 2 TEM micrograph of biomineralized RGDE8 flagella in supersaturated HAP solution for 6 days. In the selected area electron diffraction (SAED) pattern, the presence of the (211), (002) and (004) planes indicated that the HAP polycrystalline mineral nucleated on the surface of flagella. There are also some bundle-like structures as marked by circles due to the further self-assembly of flagella in the solution, which are consistent with AFM observation.

adhere and remain viable. As a well-known integrin-binding peptide, RGD is ubiquitous in many ECM proteins (*e.g.*, collagen, fibronectin, and vitronectin) that can promote cell attachment and adhesion.[24] Our data show that the display of RGD peptide on the flagella highly improved the cell spreading on their surface.

Scanning Electron Microscopy (SEM) also revealed a similar morphology of BMSCs on the different substrates (Fig. 1B). The cells were flat and stretched on the polylysine control substrates but spread less on the flagella coated substrates, especially on WT flagella. Consequently, the surface area of BMSCs decreased on the flagella-coated substrates (Fig. 1C). This is consistent with previous report of cellular morphologies on the nano-fibrous scaffolds.[25] The cells were attached on the flagella-coated substrates *via* filopodia-like extensions and exhibited more and longer ones on the M-RGDE8 flagella-coated substrates (Fig. 1B and Fig. S2, ESI†). The increased surface roughness and structural complexity after mineralization on the flagella could induce more and longer filopodia-like extensions. More compact but rough surfaces were observed on the M-RGDE8 flagella-coated substrates due to the nucleation of HAP nanocrystals (Fig. 1B, inset), which is consistent with AFM observation (Fig. 1A).

The growth rate of BMSCs was significantly altered due to the peptide display and mineralization on the flagella, as well as the unique nanotopography of the flagella (Fig. 1D). Significant higher growth rates of the cells were observed on the RGDE8-displaying flagella but slightly decreased after biomineralization. The decreased proliferation rates of BMSCs were also observed on the biomimetic mineralized collagen membranes with nanostructures.[26] As a highly osteoconductive material, HAP promotes cell differentiation and is often used in hard tissue regeneration.[27–29] After biomineralization of flagella, a high proportion of cells were induced to undergo a differentiation pathway, and thus proliferation

rates of the cells were limited.[30] Another possibility is that some of the RGD epitopes on the flagellar surface may be embedded underneath mineral layers and become unavailable to the cells. The proliferation rates of cells were significantly limited on the WT flagella-coated substrates due to the lack of bioactive signals. In another word, the display of RGD ligand with a high density on the flagella highly improved the biocompatibility of flagella-coated substrates. Because polylysine can promote cell attachment and proliferation by altering the negatively charged surface to positive,[31] as expected, we observed a higher growth rate of BMSCs on polylysine surface.

To determine BMSCs' differentiation towards osteoblasts on the flagella based substrates in osteogenic medium, the production of two bone-specific marker proteins, including osteopontin (OPN) and osteocalcin (OCN), were monitored by immunofluorescence (Fig. 3A). It has been found that the surface chemistry and nanotopography can direct both the initial cell adhesion and the differentiation signaling pathways, depending on the organization and density of functional groups on the substrate.[1,7] Peptide display enables precise control of flagella functionality through homogeneous surface modification with multivalent ligands and nanoscale distance.[17] On both day 7 and day 21, the expression of OPN for different groups was found to be in the order of M-RGDE8 > RGDE8 > WT > Con. OCN showed a similar trend although it is not as obvious as OPN. Overall the immunofluorescence data showed that WT flagella could promote osteogenic differentiation and sequential addition of RGDE8 (by genetic display) and HAP (by mineralization) onto WT flagella further enhanced such promotion effect.

The effects of surface chemistry and nanotopography of flagella on the osteogenic differentiation of cells were also measured by real-time quantitative PCR (RT-qPCR) analysis. The gene expression levels of selected osteogenesis specific gene markers (OCN, OPN, and Runx2) and non-specific gene marker (type I collagen) were detected at different time points during osteogenic differentiation for all flagella-bearing substrates (Fig. 3B), suggesting that flagella could promote osteogenic differentiation. Because the differentiation markers almost had no expression on day 1, gene expression of the cells for each marker was normalized to that on polylysine coated substrate on day 7. On day 7, the expression of the four osteogenesis specific gene markers showed the order of M-RGDE8 > RGDE8 > WT > Con, consistent with the immunefluorescence characterization of the OCN and OPN markers at the protein level (Fig. 3A). These results indicated that the differentiation of BMSCs toward osteoblasts was accelerated on the RGDE8 flagella compared to the WT flagella. RGD ligands with nanoscale distribution and lower spacing were known to enhance osteoblast proliferation and differentiation.[24,32] Apparently, the high density of RGD ligands with nanoscale spacing on the flagellar surface highly promoted early expression of osteogenic marker genes. Due to the biomeneralization of RGDE8 flagella, the nucleated HAP nanocrystals on the flagellar surface further promoted early expression of the osteogenic marker genes. After BMSCs were cultured for 21 days, the M-RGDE8 still kept a significantly higher level of osteogenesis-specific genes (OPN and Runx2) than the other groups. The level of the osteogenesis-specific
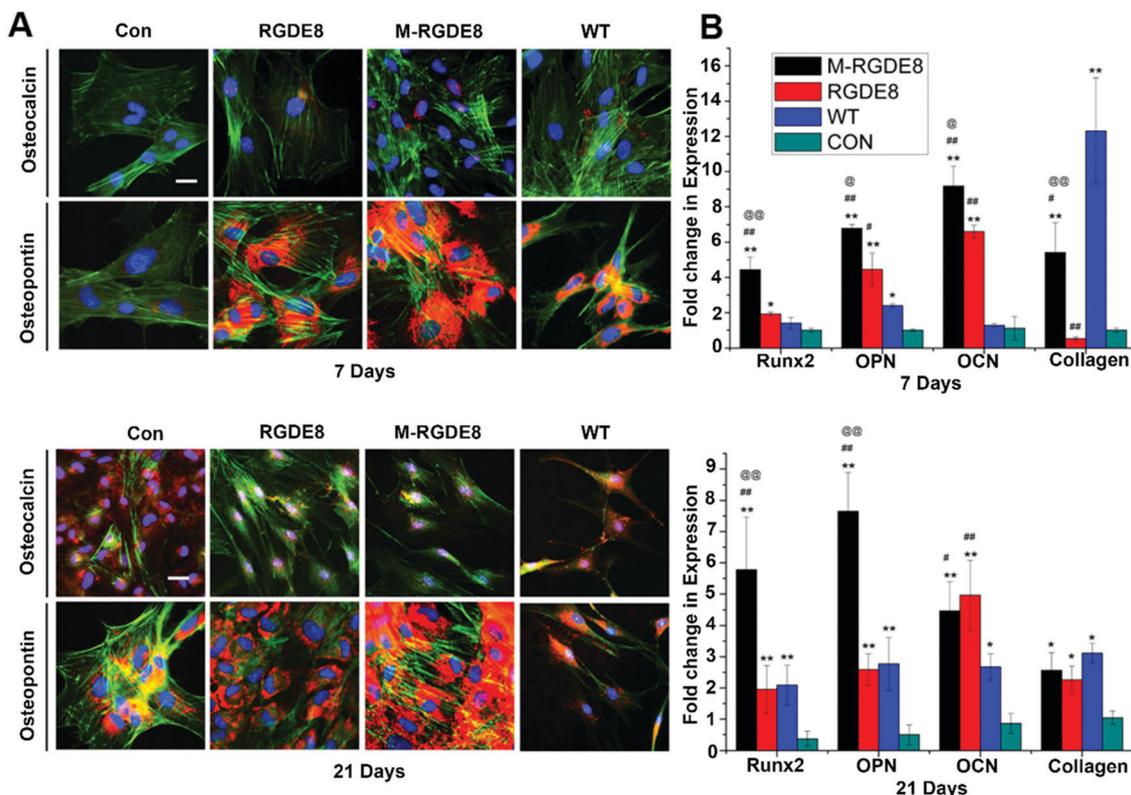
Fig. 3 Osteogenic differentiation of BMSCs examined by RT-qPCR for 7 and 21 days. (A) Immunofluorescence analysis of gene expression of OPN and OCN by BMSCs on different substrates. Color representation: cell nuclei are stained by DAPI (blue) and the F-actin of cells are stained by FITC-labeled phalloidin (green), OPN and OCN are stained by rhodamine-labeled antibody (red) (scale bar: 25 μm). (B) Quantitative analysis of gene expression of Runx2, OPN, OCN and type I collagen (Col I) at different time points. Flagella-bearing substrates can stimulate and enhance Runx2, OPN, OCN and Col I mRNA expression compared to control (compared with control group, $*p < 0.05$, $**p < 0.01$; compared with WT group, $\#p < 0.05$, $\#\#p < 0.01$; compared with RGDE8 group, $@p < 0.05$, $@@p < 0.01$).

genes (OPN and Runx2) on the RGDE8 and WT flagella substrates, though lower than that of the M-RGDE8 flagella substrate, is significantly higher than the control polylysine substrate. For OCN, M-RGDE8 and RGDE8 presented a significantly higher level than WT flagella, which exhibited a significantly higher level than the control polylysine substrate. As for the non-specific marker (type I collagen), the flagella-containing groups demonstrated a higher level than the control polylysine substrate. It is well known that the polylysine substrates could improve osteogenesis.[31] Our flagella-bearing matrix showed even higher capability in promoting osteogenesis.

Calcium-containing mineral deposits are also important markers of osteogenic differentiation. The self-mineralized calcium deposits represent the final stages of osteogenic differentiation. Alizarin red stain was used to observe the presence of calcium-containing minerals. The highest density of calcified nodule-like structures in M-RGDE8 indicated that calcium deposition was significantly enhanced in M-RGDE8 (Fig. 4A). The calcium-containing mineral deposits were also detected on RGDE8 and WT with RGDE8 bearing more deposits than WT. On control substrate, however, more fibroblast-like cells were detected. Quantitative analysis also revealed extracellular calcium deposits (nodules of mineralization) were highly increased on flagella scaffolds with an order of M-RGDE8 > RGDE8 > WT > Con.

After mineralization, a much higher number of calcified nodule-like structures were detected (Fig. 4B). The results from Alizarin red stain assay are generally consistent with those from the RT-qPCR and immunefluorescence assay. Collectively, they show WT flagella could promote osteogenic differentiation of BMSCs as compared to the substrates without flagella. Moreover, when RGDE8 was displayed on the flagella, the resultant substrates further enhanced the promotion effect. Eventually, when the HAP minerals are coated on the RGDE8 flagella by biomimetic mineralization, the resultant M-RGDE8 flagella more significantly enhanced the promotion effect than the RGDE8 flagella.

In addition to the surface chemistry, the nanotopography due to the filamentous nature and mineralization of flagella should also get involved in regulating cell behavior such as the cell morphology and anchorage, proliferation and differentiation. The less spreading of BMSCs on the flagella-bearing substrates than on the polylysine substrates could also be attributed to the nanotopography on the nanofibrous surfaces.[25] Moreover, the expression of osteogenic marker genes is sensitive to surface nanotopography. The topography of nanostructures had significant effects on osteogenesis of human mesenchymal stem cell (hMSCs) by triggering speedy expression of osteo-specific markers and enhancing osteogenic differentiation.[2,33] The nanostructured scaffolds could absorb more proteins such as fibronectin from cell culture media and,
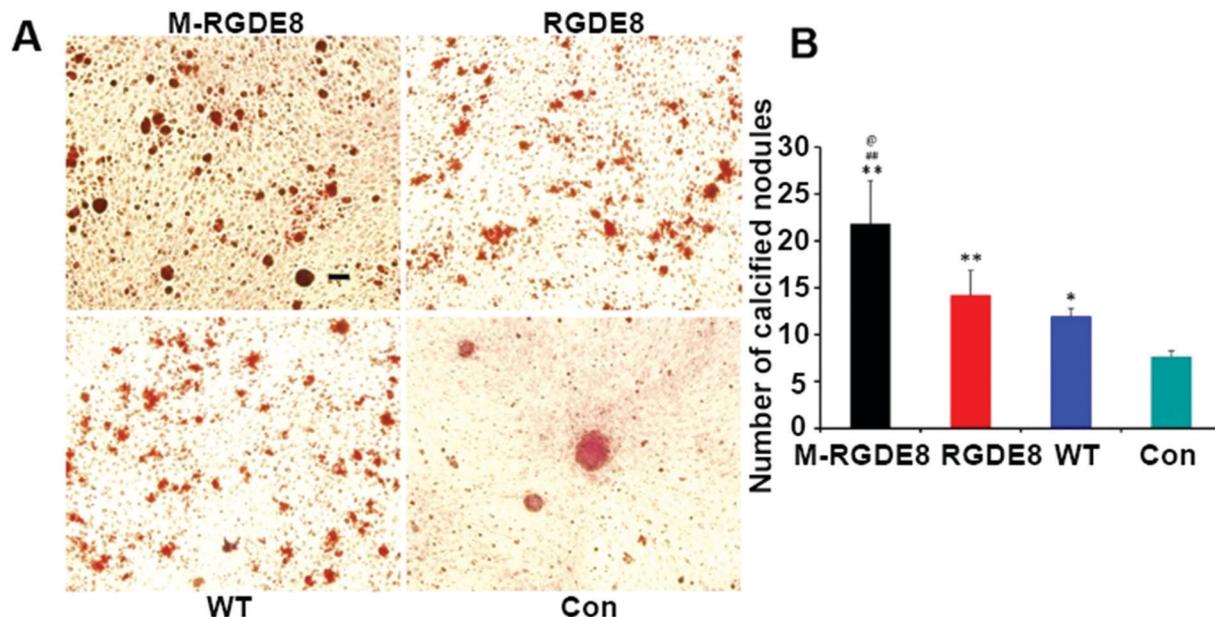
Fig. 4 Calcium-containing minerals detection. (A) The presence of calcium-containing minerals examined by Alizarin red S on different substrates. Increased density of red color was observed on the flagella-bearing scaffold, especially on the mineralized flagella. Scale bar represents 500 μm. (B) The levels of mineralization are substrate specific. A significant higher level of calcium is detected on the flagella-bearing scaffold, especially on the M-RGDE8 flagella (compared with control group,* $p < 0.05$, ** $p < 0.01$; compared with WT group, ## $p < 0.01$; compared with RGDE8 group, @ $p < 0.05$).

in turn, promoted up-regulated gene expression and increased mineralization.[21] Compared to the control non-flagella substrates, up-regulated expression of osteogenic specific markers was seen on the flagella substrates during the entire period of study. This indicated that the nanotopography of flagellar substrate should also accelerate BMSCs differentiation toward osteoblastic lineage.

The flagella are chemically stable at various conditions (*e.g.*, under the pH values ranging from 2 to 10) and quite rigid because they have a Young's modulus of $\sim 10^9$ Pa.[17,34] *FliC has* been used as radioprotective drugs *in vivo*.[35] In addition, as long as 302 amino acids can be inserted into the hyper variable region of *FliC*, which allows us the flexibility in the selection of functional motifs or their combination to be presented on the flagella.[17] These characteristics of flagella make them suitable for use as a building block in generating biomaterials.

Conclusions

In conclusion, we employed bioengineered bacterial flagella to fabricate an ECM-like matrix by a layer-by-layer assembly approach. This matrix mimics some key features of bone architecture. The HAP nanocrystals nucleated on flagella resemble minerals in bone and the RGD-displaying flagella mimic collagen fibrils. The novel genetically engineered flagella can support the adhesion and proliferation of BMSCs, indicating surface peptide or protein motifs of the bioengineered flagella can be recognized by BMSCs. The uniformly displayed functional motifs on the surface of flagella with multivalent ligands and nanoscale distance could highly up-regulate osteogenic differentiation and early maturation of the cells to the osteoblast-like cells. After biomineralization, the expression

of osteogenic markers was further increased and kept at a high level during the entire cell culture time. The biomimetic mineralized matrix derived from genetically engineered flagella incorporated with bioactive motifs and bone minerals could be a promising osteogenic biomaterial. In essence, the flagella represent a new type of nanoscale osteogenic differentiation promoters.

Conflicts of interest

There are no conflicts to declare.

Acknowledgements

Notes and references

1 A. M. Kushner and Z. Guan, *Angew. Chem., Int. Ed.*, 2011, **50**, 9026–9057.
2 L. Zhang and T. J. Webster, *Nano Today*, 2009, **4**, 66–80.
3 S. Gomes, I. B. Leonor, J. F. Mano, R. L. Reis and D. L. Kaplan, *Prog. Polym. Sci.*, 2012, **37**, 1–17.
4 R. E. Abouzeid, R. Khiari, D. Beneventi and A. Dufresne, *Biomacromolecules*, 2018, **19**, 4442–4452.
5 P. Gupta, M. Adhikary, M. J. Christakiran, M. Kumar, N. Bhardwaj and B. B. Mandal, *ACS Appl. Mater. Interfaces*, 2016, **8**, 30797–30810.

6 G. Z. Yu, D. T. Chou, D. Hong, A. Roy and P. N. Kumta, *ACS Biomater. Sci. Eng.*, 2017, **3**, 648–657.

7 A. George and S. Ravindran, *Nano Today*, 2010, **5**, 254–266.

8 M. Heim, D. Keerl and T. Scheibel, *Angew. Chem., Int. Ed.*, 2009, **48**, 3584–3596.

9 J. D. Hartgerink, E. Beniash and S. I. Stupp, *Science*, 2001, **294**, 1684–1688.

10 Y. J. Shuai, C. B. Mao and M. Y. Yang, *ACS Appl. Mater. Interfaces*, 2018, **10**, 31988–31997.

11 K. S. Sunderland, M. Y. Yang and C. B. Mao, *Angew. Chem., Int. Ed.*, 2017, **56**, 1964–1992.

12 B. R. Cao, M. Y. Yang and C. B. Mao, *Acc. Chem. Res.*, 2016, **49**, 1111–1120.

13 T. Elsdale and J. Bard, *J. Cell Biol.*, 1972, **54**, 626–637.

14 K. J. C. van Bommel, A. Friggeri and S. Shinkai, *Angew. Chem., Int. Ed.*, 2003, **42**, 980–999.

15 K. Yonekura, S. Maki-Yonekura and K. Namba, *Nature*, 2003, **424**, 643–650.

16 R. M. Macnab, *Annu. Rev. Microbiol.*, 2003, **57**, 77–100.

17 B. Westerlund-Wikstrom, *Int. J. Med. Microbiol.*, 2000, **290**, 223–230.

18 J. D. Termine, *Non-Collagen Proteins in Bone*, John Wiley & Sons, Ltd., 2007.

19 D. Li, S. M. Newton, P. E. Klebba and C. Mao, *Langmuir*, 2012, **28**, 16338–16346.

20 M. I. Setyawati, J. Xie and D. T. Leong, *ACS Appl. Mater. Interfaces*, 2014, **6**, 910–917.

21 A.-W. Xu, Y. Ma and H. Calfen, *J. Mater. Chem.*, 2007, **17**, 415–449.

22 C. B. Mao, H. D. Li, F. Z. Cui, Q. L. Feng and C. L. Ma, *J. Mater. Chem.*, 1999, **9**, 2573–2582.

23 C. B. Mao, H. D. Li, F. H. Cui, C. L. Ma and Q. L. Feng, *J. Cryst. Growth*, 1999, **206**, 308–321.

24 R. G. LeBaron and K. A. Athanasiou, *Tissue Eng.*, 2000, **6**, 85–103.

25 L. A. Smith, X. H. Liu, J. A. Hu and P. X. Ma, *Biomaterials*, 2010, **31**, 5526–5535.

26 A. Bernhardt, A. Lode, S. Boxberger, W. Pompe and M. Gelinsky, *J. Mater. Sci.: Mater. Med.*, 2008, **19**, 269–275.

27 A. Merzlyak, S. Indrakanti and S. W. Lee, *Nano Lett.*, 2009, **9**, 846–852.

28 D. A. Wahl and J. T. Czernuszka, *Eur. Cells Mater.*, 2006, **11**, 43–56.

29 N. M. Alves, I. B. Leonor, H. S. Azevedo, R. L. Reis and J. F. Mano, *J. Mater. Chem.*, 2010, **20**, 2911–2921.

30 A. W. Ettinger, M. Wilsch-Brauninger, A.-M. Marzesco, M. Bickle, A. Lohmann, Z. Maliga, J. Karbanova, D. Corbeil, A. A. Hyman and W. B. Huttner, *Nat. Commun.*, 2011, **2**, 503.

31 D. Galli, L. Benedetti, M. Bongio, V. Maliardi, G. Silvani, G. Ceccarelli, F. Ronzoni, S. Conte, F. Benazzo, A. Graziano, G. Papaccio, M. Sampaolesi and M. G. Cusella De Angelis, *J. Biomed. Mater. Res., Part A*, 2011, **97**, 118–126.

32 K. Y. Lee, E. Alsberg, S. Hsiong, W. Comisar, J. Linderman, R. Ziff and D. Mooney, *Nano Lett.*, 2004, **4**, 1501–1506.

33 M. J. Dalby, N. Gadegaard, R. Tare, A. Andar, M. O. Riehle, P. Herzyk, C. D. W. Wilkinson and R. O. C. Oreffo, *Nat. Mater.*, 2007, **6**, 997–1003.

34 H. Hoshikawa and R. Kamiya, *Biophys. Chem.*, 1985, **22**, 159–166.

35 L. G. Burdelya, V. I. Krivokrysenko, T. C. Tallant, E. Strom, A. S. Gleiberman, D. Gupta, O. V. Kurnasov, F. L. Fort, A. L. Osterman, J. A. DiDonato, E. Feinstein and A. V. Gudkov, *Science*, 2008, **320**, 226–230.